applied sciences

MDPI

Article

A Fractional-Order Creep Model of Water-Immersed Coal

Gen Li [1], Qiqi Wanyan [2,*], Zhengsheng Li [1], Haiyang Yi [1], Fengfei Ren [1], Zheng Chen [1] and Yang Liu [3]

[1] School of Mine Safety, North China Institute of Science and Technology, Langfang 065201, China; ligendc@gmail.com (G.L.); lizhengsheng0512@163.com (Z.L.); haiyangyi@ncist.edu.cn (H.Y.); r123451232022@163.com (F.R.); yqz16286248@126.com (Z.C.)
[2] Research Institute of Petroleum Exploration and Development, Beijing 100083, China
[3] School of Mechanics and Engineering, Liaoning Technical University, Fuxin 123000, China; liuyang940131@163.com
* Correspondence: wanyanqq@petrochina.com.cn

Abstract: The long-term stability of a coal pillar dam is a serious concern for coal mine underground reservoirs because of the creep behavior of coal in complex water immersion and mechanical environments. In order to investigate the characteristics of creep deformation of water-immersed coal and develop a proper creep model, this paper implemented a series of creep experiments of coal via multistage loading at various water-immersion times. The experiment data were analyzed, in terms of immersion-induced damage, elasto-plastic performance, creep behavior, etc., suggesting obvious mechanical properties' degradation of coal by water. The elastic modulus and peak strength of water-immersed coal decrease exponentially with the immersion time, while the creep rate of coal shows an upward tendency with the promoted immersion time. According to the remarked relationships of elastic, viscoelastic, and viscoplastic properties versus the stress levels and water-immersion time, a creep model based on conformable fractional derivatives is proposed, considering the influence of the water-immersion time and variable stress level. The proposed model was verified using the experiment data, showing a good capacity of the creep model for reproducing the creep process of water-immersed coal. This paper provides a fundamental model for further studying the stability of coal pillars and their influence on the safety of underground water reservoirs.

Keywords: immerse coal; creep behavior; constitutive model; fractional order; parameter correction

check for updates

Citation: Li, G.; Wanyan, Q.; Li, Z.; Yi, H.; Ren, F.; Chen, Z.; Liu, Y. A Fractional-Order Creep Model of Water-Immersed Coal. *Appl. Sci.* **2023**, *13*, 12839. https://doi.org/10.3390/app132312839

Received: 27 September 2023
Revised: 24 November 2023
Accepted: 27 November 2023
Published: 29 November 2023

Copyright: © 2023 by the authors. Licensee MDPI, Basel, Switzerland. This article is an open access article distributed under the terms and conditions of the Creative Commons Attribution (CC BY) license (https://creativecommons.org/licenses/by/4.0/).

1. Introduction

The coal pillar dam is an important part of coal mine underground reservoirs (CUR) [1–3], which isolate the various water purification areas and support the overburden rock [4,5]. In such a complex environment, the coal pillars are usually subjected to a hydro-mechanical-chemical coupled process. Since coal has significant creep behavior, especially in the water-immersed conditions [6–8], if creep-induced instability occurred in coal pillars, the supporting and isolating effects of the coal pillar will disappear, consequently destroying the CUR; therefore, the long-term stability of the coal pillar dam is a serious concern for CUR.

Research on the short-term stability of CUR is numerous and great success has been achieved using innovative techniques [9–12]. In recent years, the long-term performance of CUR, especially concerning the coal pillars of CUR, aroused great interest in the research community because of the safety issue brought by the impact of circular flooding and water-immersion to coal pillars [13]. Evidence from the laboratory suggests that water immersion has a significant influence on the mechanical performance of coal [14,15] because of the water-softening effect on the coal rock [16,17]. Based on the acoustic emission features of the coal-rock combined samples under different immersion durations, refs. [18–21] found that water has a deteriorating effect on the mechanical properties of the coal-rock combined samples as well.

In the work of a stability assessment of the coal pillars in a CUR, a proper creep model of coal rock is a priority for numerical modeling or calculating works. Currently, the majority of research is focused on how the water content affects coal strength, whereas there is still a lack of studies on the coal creep process in water-immersion conditions [22,23]. In practical engineering, coal pillar dams are often exposed to groundwater immersion for a long period of time, leading to creep under the overburdened rock [24–26]. In order to accurately describe the creep performance of coal columns under the influence of the softening effect of water immersion, it is necessary to establish a suitable creep model for water-immersed coal, which reflects the deformation characteristics of coal at various stages.

According to the summary of [27], the creep constitutive model for rock materials has three types, namely, empirical models, component models, and mechanism-based creep constitutive models. Empirical models are derived from experimental observations, which are usually expressed by a power law or an exponential function [28]. However, the difference in time scale between an experimental study and a practical engineering project leads to an error between the predicted and measured creep deformations [29,30]. The classic component combination models include the Maxwell model, the Kelvin model, the Bingham model, the Burgers model, and the Nishihara model, with clear physical meanings [31,32]. Considering the creep damage accumulation, mechanism-based creep models are commonly established according to the viscoelastic and viscoplastic behavior of rock during the creep process [33–35].

On account of the complex nonlinear behavior of creep deformation in rock materials, the fractional derivative theory was introduced into the creep model, where Zhou et al. [27,36] proposed a creep constitutive model based on the fractional derivative with an Abel damper instead of a Newton damper, which well reflects the three stages of salt rock, especially the accelerated creep stage. Zhang et al. [37] developed a fractional derivative constitutive model to describe the creep process of deep coal rock, which depicts well the accelerated creep stage. Deng et al. [38] proposed a fractional-order creep model of coal and rock to characterize the changes in each loading stage.

In summary, previous studies on the constitutive relationship of coal-rock creep, especially the introduction of fractional derivatives, makes it possible to accurately describe the full stages of rock creep, of which this creep constitutive equation of coal and rock is studied in different ways, and the constitutive equation is established based on the influence of damage, water content, temperature, stress, and other factors. However, the factor of water-immersion time is less considered in the fractional creep constitutive model of rocks for CUR.

Therefore, in order to develop a proper model that considers the influence of the water-immersion effect, aiming at providing a foundation for the assessment of coal pillar stability and water sealing performance, on account of the softening effect of coal under different immersion durations, this paper conducts a uniaxial multistage creep experiment of coal at different water-immersion times, then analyzes the influence of water-immersion on the creep properties of coal based on the experiment results. According to the evolutionary relationship between the creep properties of coal and water-immersion time, a fractional derivative-based creep model is developed with the variables of immersion time and stress level. The proposed creep model of this paper will provide a theoretical basement for further study on the stability of coal pillars and overburden rock layers induced by the continuous creep failure of coal pillars.

2. Experimental Methods

In order to develop the creep model of coal while also considering the factors of the water-immersion time, water-immersion experiments and multistage creep experiments were involved in this paper. The water-immersion experiments aim at preparing immersed samples with the target immersion times for the multistage creep experiments.

2.1. Specimen Preparation

The tested samples were picked from the Lingxin Coal Mine, which is located in an extremely water-deficient area of western China. This coal mine is being constructed as a demonstration project of CUR with an attempt to improve the utilization of mine water in this area.

The concept of the experiment involved in this paper aims at understanding the law of the creep performance of water-immersed coal; therefore, the standard coal sample should be prepared firstly by core drilling, cutting, and polishing. Then, water immersion on these samples should be implemented to the target time, and after that is the creep experiment of the immersed coal samples under various durations. The SCQ-300-type automatic stone cutting machine (XinChuan Intelligent Corporation, Suzhou, China), SC-200-type automatic core drilling machine (XinChuan Intelligent Corporation, Suzhou, China), and M250-type surface grinding machine (XinChuan Intelligent Corporation, Suzhou, China) were employed to make the specimen have cylindrical-shaped dimensions with a diameter of 50 mm and a height of 100 mm, as shown in Figure 1a. The processed coal specimens were measured and weighed using electronic vernier calipers and high-precision 7-degree electronic scales, as shown in Figure 1b. The coal samples with similar weights and sizes within the error range were selected as experimental ones. In addition, all the specimens were ensured that the non-parallelism of the two ends of the specimen were $\leq$0.05 mm, with an axial deviation $\leq$0.25°.

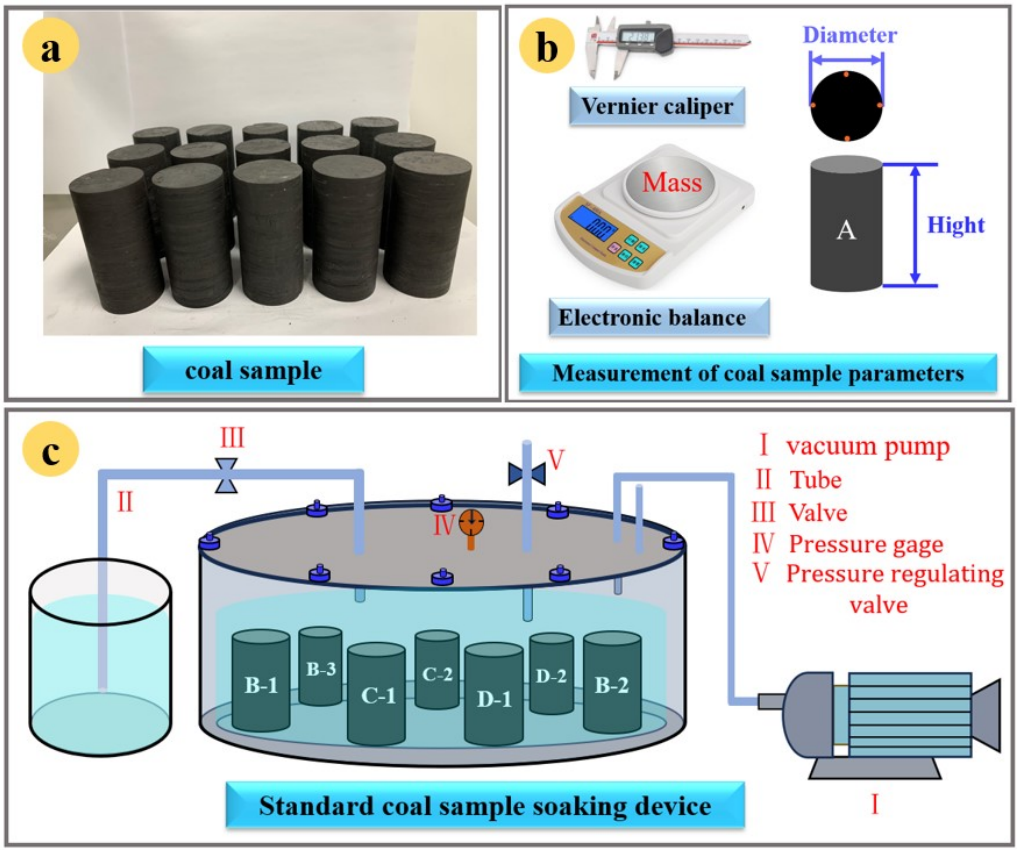


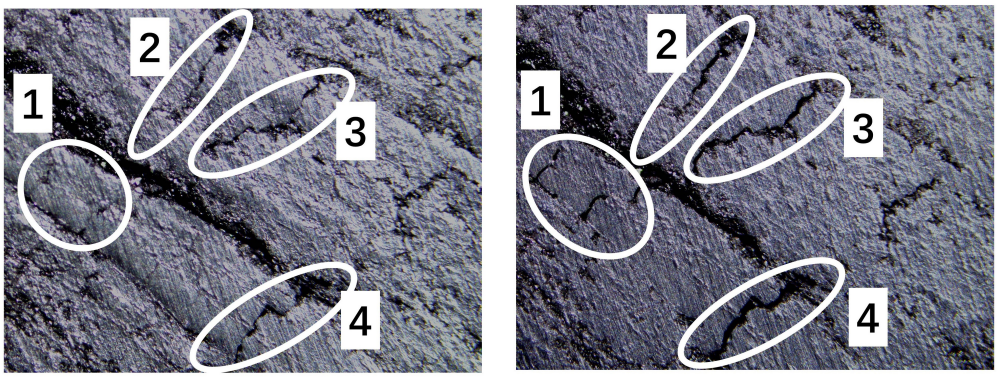
Figure 1. Coal sample soaking process with (**a**–**c**) the standard coal samples, measuring devices and water-immersion facilities, respectively.

In order to simulate the water-immersion conditions of the coal pillar dam in a CUR, the immersion experiments were carried out under constant temperature in a vacuum saturation chamber. Specifically, as shown in Figure 1c, all the specimens were firstly put into a vacuum drum and pumped to the vacuum state, then the natural water was injected into the vacuum drum via a conduit until the coal samples were completely immersed.

After that, the vacuum drum was opened at the target times. Three groups with seven pieces of the coal samples in total were immersed at different durations as follows: specimen B was immersed for 7 days, specimen C was treated for 14 days, and specimen D was immersed continuously for 30 days. A specimen named A was an unimmersed specimen.

2.2. Structural Observation of Immersed Coal

The softening effect of water on coal is mainly due to the dissolution of water on the microstructure of coal [39]. Many scholars have pointed out that coal undergoes corrosion effects and crack propagation during immersion [22,40,41]. This paper conducted structural observation in the coal immersed for 14 days with a microscope magnification of 100×. As shown in Figure 2, despite the limited resolution, changes in the crack state are obvious after water immersion, exhibiting a crack width which is expanded and slightly propagated.



(**a**) (**b**)

Figure 2. Microscopic image of coal dissolution (**a**) before immersion; (**b**) after immersion.

The deterioration of coal's mechanical properties will seriously damage its long-term creep performance [42,43], which is almost fatal to the coal pillars of underground reservoirs in coal mines. Therefore, it is necessary to carry out long-term creep experiments of water-immersed coal, understand the evolutionary creep performance of coal after immersion, and put forward a suitable creep model for coal pillars in underground reservoirs, so as to better describe and predict the creep stability of coal pillars. This will be beneficial to researchers and designers on account of the long-term safety of underground reservoirs in coal mines.

2.3. Experimental Facilities

The creep experiment was implemented using the long-term creep test machine, as displayed in Figure 3, which is self-developed by the Institute of Petroleum Exploration and Development. The creep test equipment includes an axial loading system, a pressure control system, a deformation monitoring system, and a computer control system. This experimental machine can carry out rock mechanics experiments under uniaxial compression and tension, relaxation, creep, cyclic, and other loading paths; the loading program can be adjusted according to the experimental needs; and the axial pressure and loading time can be adjusted. The frame stiffness reaches 2×10^7 kN/m and the maximum test force is 2000 kN, which meets the research needs.

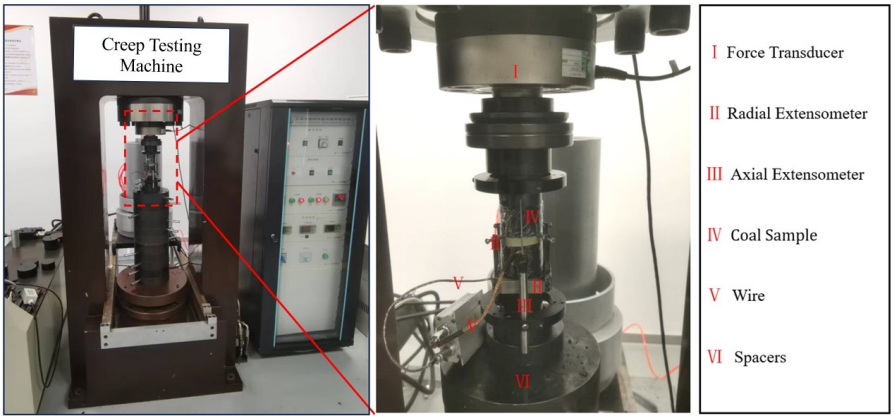


Figure 3. Facilities of creep experiment.

In order to avoid the influence of the external environment, the whole set of experimental equipment is placed at a constant temperature at 20 °C. The axial and radial deformation of the sample was measured using an extensometer and the axial force was measured according to a force sensor. Force controlling is adopted as the loading method and real-time data is collected throughout the loading process. The creep experiments applied a graded loading method, where the initial stage is 3 MPa and the loading increment for each stage is 2 MPa. The loading rate is set as 0.001 MPa/S, the duration of each stage is 24 h, and the final stage loading time was determined by the failure time of the tested sample.

2.4. Results of Creep Deformation

All the measured data of creep strain versus time is plotted in Figure 4. Each loading stage, as shown in the subfigure in Figure 4, experienced instantaneous creep deformation, as well as decelerating, steady, and accelerating creep at the last loading stage. As announced by [32], under the axial load, the coal sample experiences an instantaneous elastic strain, during which the internal pores of the coal are compacted, resulting in significant deformation. Subsequently, the sample enters the decelerating creep deformation, characterized by a convex creep curve, indicating an increase in strain with a decreasing creep rate as the internal pores continue to be compacted. Once the creep rate reaches a certain level, it remains constant, known as the steady creep stage, where creep strain exhibits a proportional relationship with time. Finally, the sample enters the accelerating creep stage, which occurs for a short period, and the creep strain increases approximately exponentially with time.

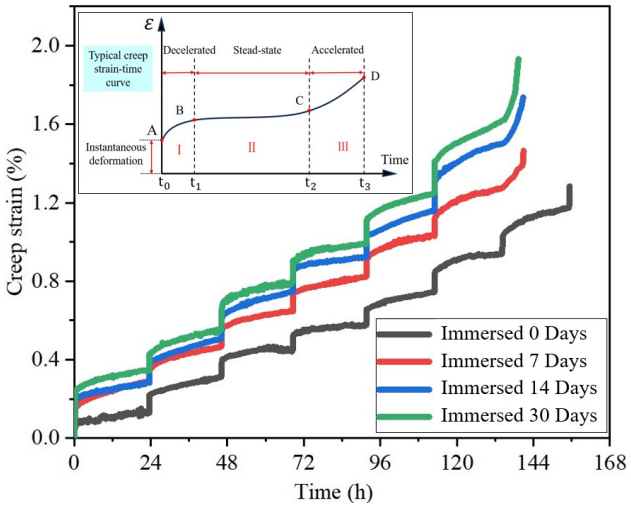


Figure 4. Strain–time curves of experimental specimen.

As shown in Figure 4, a significant difference can be seen from the strain versus time curves of the coal samples with different immersion times. Under the same stress level, the longer the immersion time of the sample, the more severe the deformation. This indicates that the water immersion has a softening effect on the strength of the coal. In addition, it can be found that for the same experimental coal sample, when the horizontal stress rises, the deformation generated by the coal sample becomes more obvious and the creep stress changes greatly. This indicates that the increase in stress has a promoting effect on the creep of coal, which can accelerate the creep of coal. When the load is greater than the yield strength of coal and rock, the internal pores and cracks of the material will have a large range of penetration and the coal and rock will fail after the deformation reaches a certain value. This stage can be called the accelerated creep stage or plastic failure stage. Immersed samples D, C, and B enter the accelerated creep stage according to the length of the immersion time when the loading stress is 13 MPa, while the non-immersed sample A enters the accelerated creep stage when the loading stress is 15 MPa, indicating that the coal rock has a softening effect after immersion.

To investigate the influence of immersion time on the creep behavior, the time–strain curve of the coal sample under different immersion durations is compared in Figure 4. The deformation of the soaked coal sample is significantly greater than that of the non-soaked coal sample and the rate enters the plastic failure stage first. Moreover, the longer the soaking time of the coal sample, the greater the creep strain generated. This indicates that immersion has a significant impact on the mechanical properties of the coal sample, leading to significant differences in the creep stages of the tested coal sample. As announced by [44], water has a softening effect on coal via mineral dissolution, Rhebinder-effect-induced cohesion deduction, chemical bond-breakage-induced crack propagation, etc. In order to further study the creep performance of immersed coal, the evolution of elasticity, creep strength, and creep rate have been analyzed in the following subsections.

3. Evolution of Creep Performance

3.1. Evolution of Elastoplastic Properties

In order to analyze the elastoplastic properties of the immersed coal samples, their loading stress versus strain data during the creep experiments were assembled as the example of sample C, as displayed in Figure 5. Obviously, in the first loading stage, compaction of the sample appeared, exhibiting a curve growth gradient, despite linear growth of the measured curve data after the second loading stage, and plastic deformation was observed after about the sixth load stage, which was increasingly significant before the peak stress.

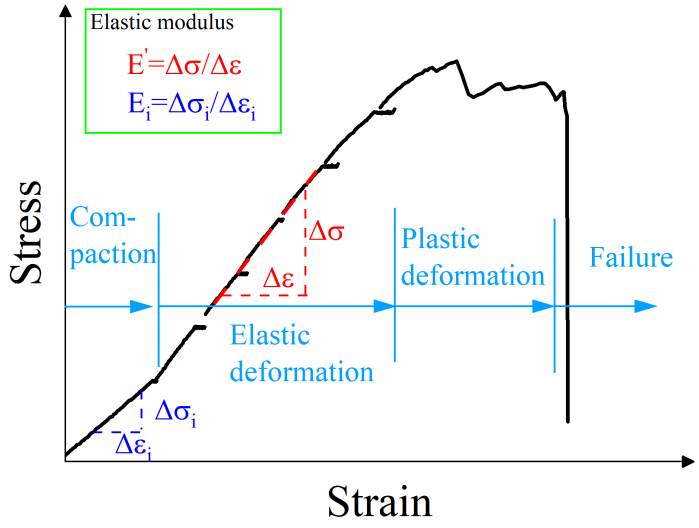


Figure 5. Curve of stress vs. strain.

The nature of the deformation of the immersed specimen at the initial loading stage is in accordance with Hooke's law as a linear elastic stress–strain relationship. The calculated elastic modulus of specimens A, B, C, and D are 5.01 GPa, 4.31 GPa, 3.79 GPa, and 3.52 GPa, respectively. As plotted in Figure 6, the data of the elastic modulus yields the fitted function with a variable of the immersion time, in which $E_0 = 5.015$ GPa, $a = 0.315$, and $\beta = 11.189$, and the residual sum of squares $R^2 = 0.98$.

The overall tendency of Figure 6 suggests that immersion time decreases the elastic modulus of coal, and with the growth of immersion time, the elastic modulus of a specimen immersed for a long period of time tends to stabilize to a steady level. That behavior is manifested in engineering as a gradual softening of the coal-rock mass with the increasing immersion time, and the immersion time has a significant effect on the mechanical properties of the coal pillar dams in underground reservoirs, which may lead to creep instability of the coal pillars.

Compared to the non-immersed sample, as plotted in Figure 6, the elastic modulus of the one immersed for 7 days decreased by about 0.70 GPa (47.37 %); the one immersed for 14 days descended by about 1.22 GPa (82.31 %); and the one immersed for 30 days has approximately a 1.48 GPa deduction in the elastic modulus. As a whole, the elastic modulus has an exponential relationship to the immersion time, which can be expressed by Equation (1), in which a and b are the coefficients and T_c means the immersion time.

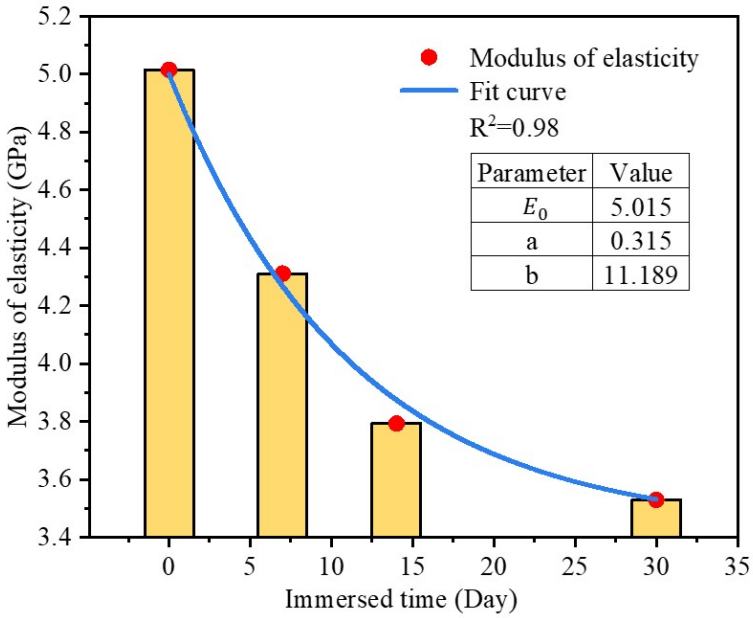


Figure 6. Curve of elastic modulus and immersion days.

$$E^* = E_0\left(1 - a\left(1 - \exp\left(-\frac{T_c}{b}\right)\right)\right) \quad (1)$$

The elastic modulus versus loading stress is displayed in Figure 7, where the compaction of the coal specimen was also observed, exhibiting the initial growth in the elastic modulus. From the second level of loading stress, despite a slight fluctuation of the calculated elastic modulus, it kept stable as the corresponding elastic region, as illustrated in Figure 5. Plastic damage appeared with the promoted loading stress, resulting in the continuous deduction of the elastic modulus in Figure 7.

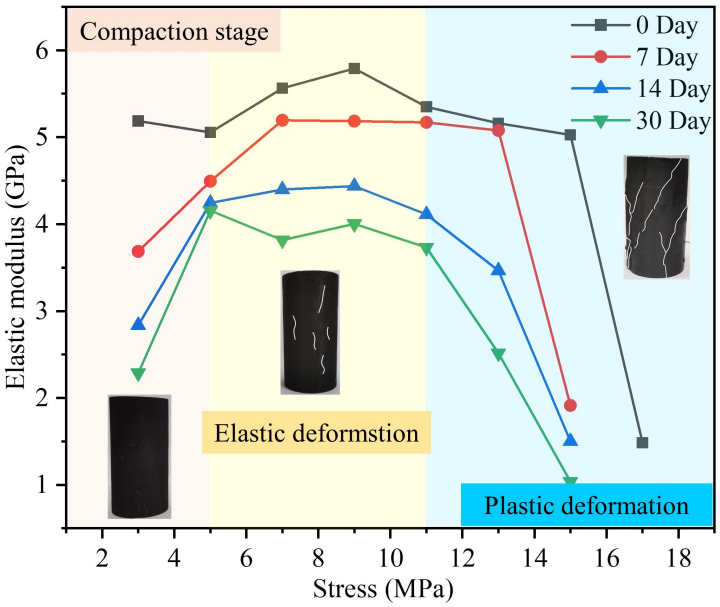


Figure 7. Elastic modulus–stress relationship curve.

It is not only the elastic modulus that was changed via water immersion but also the peak strength. As plotted in Figure 8, the peak strength of the tested specimen degraded non-linearly with the immersion time. Interestingly, such degradation tendency is similar to that of the elastic modulus in Figure 6. Therefore, a consistent formulation of the evolution of peak strength can be expressed by Equation (2), where c and d are the coefficients.

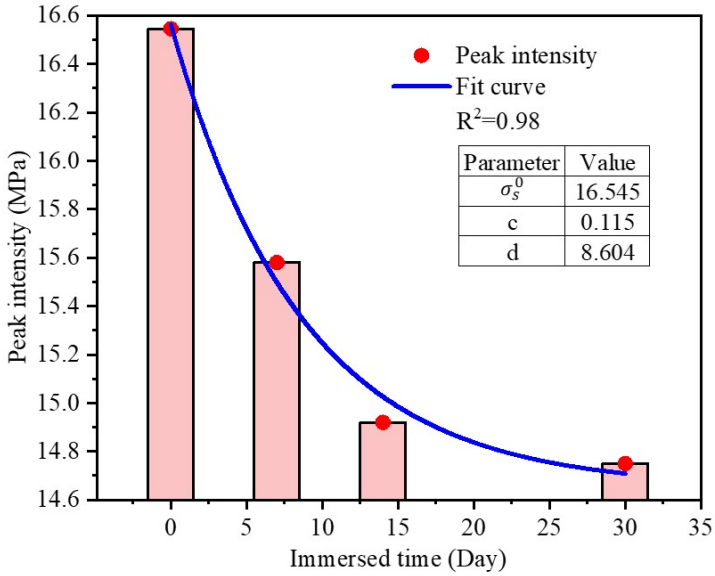


Figure 8. Peak strength–immersion time curve.

$$\sigma_s = \sigma_s^0\left(1 - c\left(1 - \exp\left(-\frac{T_c}{d}\right)\right)\right) \tag{2}$$

Under uniaxial stress state $\sigma_3 = 0, \sigma_1 = \sigma_s^0$,

$$\frac{\sigma_s^0}{2} = C * \cos\varphi + \frac{\sigma_s^0}{2}\sin\varphi \tag{3}$$

$$\sigma_s^0 = \frac{2\cos\varphi}{1-\sin\varphi} \tag{4}$$

Substitute Equation (4) into Equation (2)

$$\sigma_s = \frac{2\cos\varphi}{1-\sin\varphi} * \left(1 - c\left(1 - \exp\left(-\frac{T_c}{d}\right)\right)\right) \tag{5}$$

The above analysis convinces us that water immersion has a large impact on the elastic modulus of the coal samples, showing a gradually decreasing tendency during water immersion that is ultimately maintained near a stable value. According to reference [33], this is due to a large number of closed fissures within the coal, of which friction properties will be changed via the water immersion, thereby making the contact surface more easily undergo deformation. It indicates that water immersion has an obvious softening effect on the coal samples. In the case of a coal pillar dam, such effect leads to a large deformation of pillar compression and rock movement in the overburden layers, consequently posing a threat to the CUR via water leakage.

Additionally, the longer the immersion time, the smaller the peak intensity of the coal samples. Researchers believe that the peak strength and elastic modulus of the coal samples after immersion were reduced due to the role of water in the immersion process as a lubricant and catalyst [36], and the higher the water content of the coal samples after water saturation, the higher the degree of weakening, which is in line with the results of this paper, but the rate of decline in the peak strength decreased gradually with the growth of time, which indicates that the reduction in the peak strength of the specimen by the time of immersion is not unlimited and the longer the time of immersion, the longer the effect of water leaching on the peak strength of the coal samples showed a trend of gradual decrease. The effect of water immersion on the peak strength of the coal samples shows a trend of gradual decrease the longer the immersion time is. When the coal pillar acts as the dam of a coal mine underground water reservoir, it is necessary to fully consider the deterioration of the mechanical properties of the coal pillar dam.

3.2. Evolution of Creep Rate

3.2.1. Steady Creep Rate

In order to analyze the influence of the water-immersion time and stress level on the creep properties of the coal samples, the creep rates were calculated in this subsection. In order to obtain the steady-state creep rate of the coal samples during the constant velocity creep stage, stress levels of 5 MPa, 7 MPa, 9 MPa, and 11 MPa were selected during the graded loading processes. The steady-state creep rates of the coal samples were calculated for different immersion times and a three-dimensional scatter plot was drawn. The X-axis represents the immersion time, the Y-axis means the stress, and the Z-axis is the creep rate. The results are shown in Figure 9a. From Figure 9a, it can be observed that the loading stress and immersion time have certain effects on the creep rate. To investigate this effect, three-dimensional scatter plots are projected onto the Y-Z plane and X-Z plane, respectively.

From Figure 9b, it is not difficult to see that for coal samples A, B, C, and D with different immersion times, the creep rate of coal is positively correlated with the stress level. The higher the stress level, the faster the creep rate of coal. This indicates that applying stress can accelerate the creep of coal under the condition that the stress does not exceed the ultimate strength of the coal rock. In addition, it can be seen from Figure 9c that at the same stress level, the creep rate increases with a longer immersion time. This is mainly due to the increase in microcracks within the coal body with the increasing immersion time. When the immersion time is less than 30 days, the immersion time has a significant effect on the creep rate. After it passes 30 days, the effect of immersion time on the creep rate begins to decrease. Therefore, the creep rate increases with both the promoted stress level and immersion time.

Keeping the stress as a constant, the strain slowly increases with time, which is also known as the steady creep deformation stage. From the above analysis, it can be seen that loading stress and immersion time are the main factors affecting the coal creep rate. The steady creep rate shows an increasing trend with the increase in immersion time and loading stress, and their relationship is shown in Figure 9.

The relationship of viscoelastic strain versus stress and time, where the viscosity coefficient satisfies

$$\dot{\varepsilon}^{ve} = \frac{\sigma}{\eta_1} \tag{6}$$

Considering the evolution of the viscosity coefficient according to the surface fitting of the data of Figure 9, it results in

$$\eta_1^* = \eta_1 \exp(k_1\sigma + k_2 T) \tag{7}$$

The fitted values of η_1, k_1 and k_2 are 0.0005946, 0.00978 and 0.00419, respectively. The fitted surface is plotted in Figure 9a, where its squared residual error $R^2 = 0.88$. Despite a certain range of differences existing between the measured data and the fitted result due to the discreteness in the coal samples, the fitted surface is capable of covering the tendency as a whole.

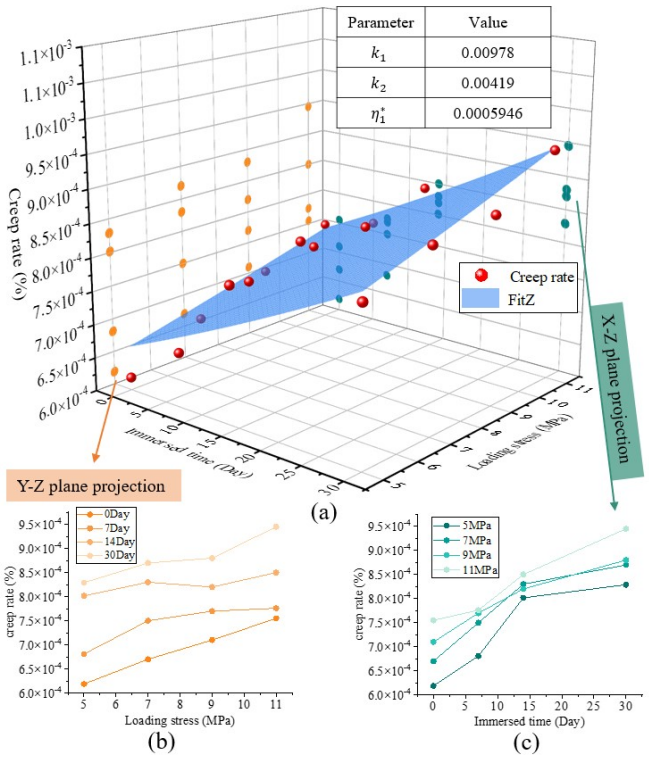


Figure 9. The curve fitting of steady-state creep rates (**a**) time-stress-creep rate; (**b**) stress-creep rate; (**c**) time-creep rate.

3.2.2. Accelerated Creep Rate

When the amount of creep load is greater than its own strength limit, the specimen enters the accelerated creep deformation stage; at this time, the damage begins to accelerate from the damage region to the surrounding integrity of the region diffusion, ultimately leading to plastic damage of the specimen, of which the accelerated creep rates of the specimen with different immersion times are shown in Figure 10. It can be seen that the longer the specimen immersion time, the faster its rate in the accelerated creep deformation stage, and the accelerated creep rates of the specimen versus the immersion time show an upward trend. The reason for this phenomenon is the softening effect that occurs after the

specimen is immersed in water, where the longer the immersion time, the more pronounced the softening effect.

Before the loading stress reaches 13 MPa, each specimen undergoes steady creep. However, as the loading stress increases, damage accumulates and the creep rate increases. Each specimen enters the accelerated creep deformation stage one by one, during which the strain rate of the specimen increases significantly. The relationship equation is as follows:

$$\dot{\varepsilon}^{vp} = \frac{(\sigma - \sigma_s)e^{\beta t}}{\eta_2^*} \tag{8}$$

During the accelerated creep deformation stage, the accelerated creep rate of specimens under different immersion times versus stress levels were fitted and the results are shown in Figure 10. The parameters obtained as $\eta_2^* = 0.000604637, m_1 = 0.01953, m_2 = 0.00783$.

$$\eta_2^* = \eta_2 \exp(m_2\sigma + m_2 T) \tag{9}$$

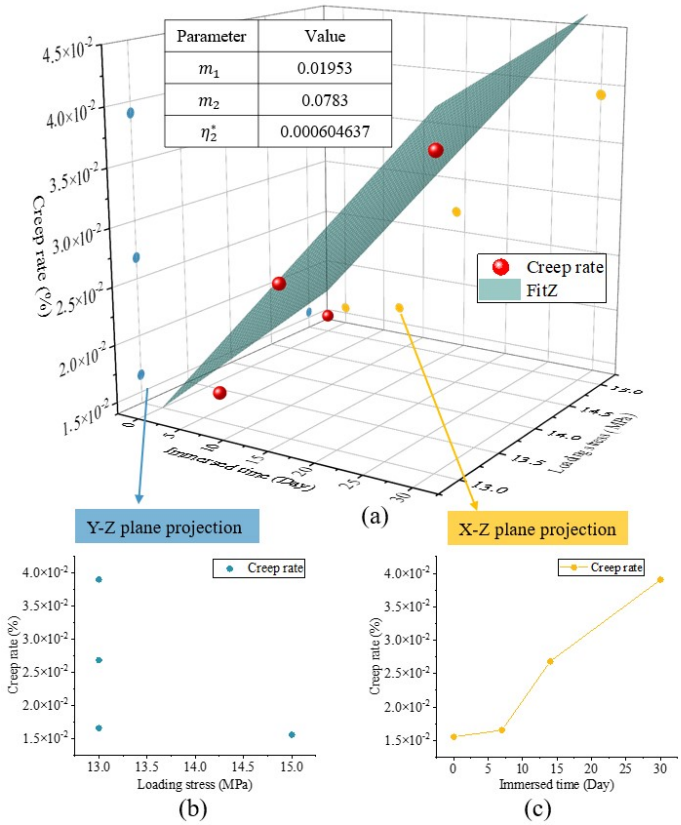


Figure 10. The curve fitting of accelerated creep rates (**a**) time-stress-creep rate (**b**) stress-creep rate (**c**) time-creep.

4. Fractional-Order-Based Creep Model

4.1. One-Dimensional Fractional-Order Creep Model

Due to the highly nonlinear characteristics presented in the creep process of coal rock, the traditional constitutive relationship based on the integer order (such as the Newtonian dashpot) in the creep element model can no longer accurately describe the characteristics of each stage of the creep process. In this paper, we transformed the integer-order derivatives in the Newtonian dashpot into fractional-order derivatives and the Newtonian kettle in the constitutive model into a fractal dashpot, as shown in Figure 11.

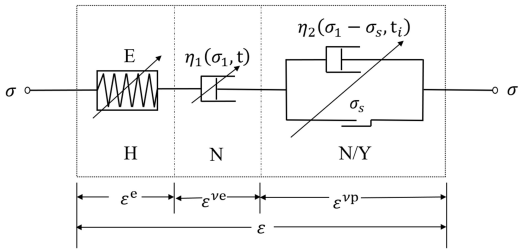


Figure 11. A conceptual creep model of water-immersed coal.

As shown in Figure 11, the proposed fractional creep model includes an elastic body (H), a nonlinear viscous body (N), and an ideal viscoplastic body (N/Y body) in series, which are used to describe the attenuated creep deformation, isochronous creep deformation, and accelerated creep stages during the graded loading of the inundated coal rock, respectively.

The fractional-order derivatives have several different definitions such as the Riemann–Liouville definition, the Caputo definition, and the Riesz potential operator, etc. The fractional-order derivatives used in this paper are the conformable derivatives proposed by Khahlil in 2014 [45]:

$$T_\alpha f(t) = \lim_{k \to 0} \frac{f\left(t + kt^{1-\alpha}\right) - f(t)}{k} \tag{10}$$

where $T_\alpha f(t)$ denotes the α-order derivative of the function f with respect to t. In addition, Khahlil gives the conformable fractional-order derivative with respect to the fractal derivative as

$$T_\alpha f(t) = t^{1-\alpha} \frac{df(t)}{dt} \tag{11}$$

The relationship between the stress and strain rate in the traditional ideal dashpot (Newtonian dashpot) can be expressed as

$$\sigma(t) = \eta \frac{d\varepsilon(t)}{dt} \tag{12}$$

where η is the coefficient of viscosity. By changing the first-order derivatives in the ideal elastic dashpot to fractional-order derivatives based on the conformable derivatives, the fractional-order dashpot based on the conformable derivatives can be obtained:

$$\sigma(t) = \eta T_\alpha \varepsilon(t) = \eta t^{1-\alpha} \frac{d\varepsilon(t)}{dt} \tag{13}$$

when the fractional-order derivative number equals 1, Equation (14) becomes the stress–strain relation $\sigma(t) = \eta \frac{d\varepsilon}{dt}$ for an ideal fluid. For the creep process, the stress is a constant σ. Substituting $\sigma(t) = \sigma$ and integrating both sides of Equation (14) yields:

$$\int d\varepsilon(t) = \int \frac{\sigma}{\eta} t^{\alpha-1} dt \rightarrow \varepsilon(t) = \frac{\sigma}{\eta\alpha} t^\alpha + C \tag{14}$$

The initial strain is 0, where one can obtain the constant $C = 0$ in Equation (15); Equation (15) portrays the power–law relationship between strain and time in a fractional-order viscous dashpot.

$$\sigma(t) = \eta_0 e^{-\beta t} \frac{d\varepsilon(t)}{dt} \tag{15}$$

where η_0 is the initial cohesion factor and β is the damage factor.

In the accelerated creep deformation stage of the coal-rock body, rupture damage occurs in the coal-rock body and it is necessary to consider the damage on the basis of the element model. According to the damage theory, the damage variable α is introduced into

the elemental model and the relational equation of the stress–strain in the creep process of the ideal viscous kettle under the consideration of damage is obtained.

For creep experiments, σ is a constant, so integrating Equation (16) yields the ideal dashpot strain–time relationship as:

$$\varepsilon = \frac{\sigma e^{\beta t}}{\eta_0 \beta} \tag{16}$$

For the proposed fractional derivative constitutive model, the first part, namely the Constitutive equation of elastic elements, can be expressed as:

$$\varepsilon_e = \frac{\sigma}{E} \tag{17}$$

where σ is the creep loading stress and E is the elastic modulus of the elastic body.

In the second part, the constitutive equation of viscous components based on uniform fractional derivatives can be expressed as:

$$\varepsilon_v = \frac{\sigma}{\eta_1 \alpha} t^{\alpha} \tag{18}$$

where η_1 is the initial viscosity coefficient of the viscous element and α is the fractional derivative, $0 < \alpha < 1$.

In the third part, the constitutive equation of the parallel model of the viscous body and plastic body considering damage can be expressed as:

$$\begin{cases} 0 & \sigma < \sigma_s \\ \varepsilon_{vp} = \frac{(\sigma - \sigma_s) e^{\beta t}}{\eta_2 \beta} & \sigma > \sigma_s \end{cases} . \tag{19}$$

where σ_s represents the plastic yield limit of the material, η_2 represents the initial viscosity coefficient of the viscous element in the parallel body, and β is the damage coefficient used to characterize the damage process. When the creep loading stress σ is less than the yield limit σ_s, the material will not exhibit viscoplastic characteristics. When the loading stress σ is greater than the yield limit σ_s, the material exhibits viscoplastic characteristics and accumulates damage.

The relationship between the total stress and total strain of the component model is:

$$\begin{aligned} \varepsilon &= \varepsilon_e + \varepsilon_v + \varepsilon_{vp} (a) \\ \sigma &= \sigma_e = \sigma_v = \sigma_{vp} (b) \end{aligned} \tag{20}$$

Therefore, by substituting Equations (16)–(19) into Equation (20), we can obtain the constitutive equation as follows:

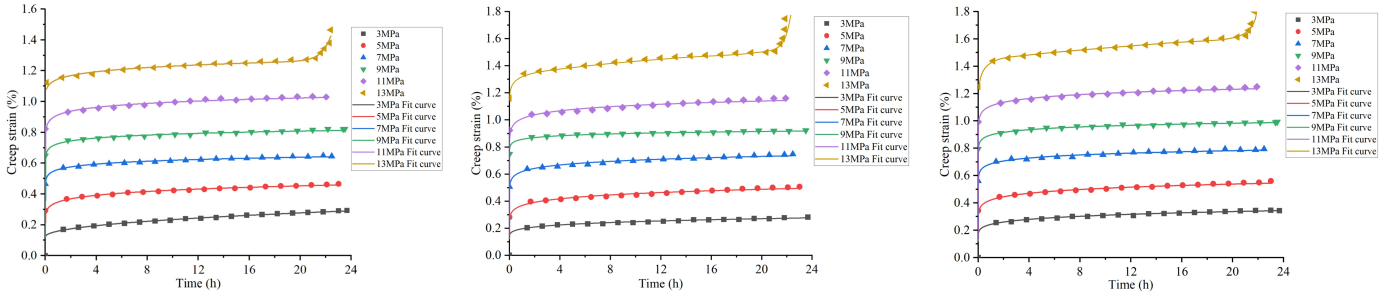
$$\varepsilon = \begin{cases} \frac{\sigma}{E} + \frac{\sigma}{\eta_1 \alpha} t^{\alpha} & \sigma < \sigma_s \\ \frac{\sigma}{E} + \frac{\sigma}{\eta_1 \alpha} t^{\alpha} + \frac{(\sigma - \sigma_s) e^{\beta t}}{\eta_2 \beta} & \sigma > \sigma_s \end{cases} . \tag{21}$$

4.2. Validation of Creep Damage Model Parameters

To validate the proposed fractional-order creep model, data fitting of the proposed model was conducted using the indoor experimental test results in Section 2. The creep test results of the coal under stress conditions of 5 MPa, 7 MPa, 9 MPa, 11 MPa, and 13 Mpa and immersion conditions of 7 days, 14 days, and 30 days were used to verify the proposed fractional-order creep model.The fitting results are shown in Figure 12. For the fitting process, this paper did not adopt different fitting parameters for specimens immersed for different durations. Instead, the three types of specimens immersed for different durations were fitted using the same set of parameters. The data fitting of the model was performed using the Origin data analysis software. The fitting parameters are shown in Table 1.

Table 1. Table of fitted parameters.

Parameters	E^*	a	b	η_1^*	k_1	k_2
Value	5.015 GPa	0.3126	11.18947	0.0005946	0.00978	0.00419
Parameters	η_2^*	m_1	m_2	σ_s^0	c	d
Value	0.000604637	0.01953	0.0783	16.56	0.1154	8.604
Fitting	R_B^2	R_C^2	R_D^2			
Value	0.85	0.86	0.83			



(**a**) (**b**) (**c**)

Figure 12. Strain–time fitting curve for (**a**) specimen immersed for 7 days; (**b**) specimen immersed for 14 days; and (**c**) and specimen immersed for 30 days.

According to Table 1, it can be seen that the proposed fractional-order constitutive model can well fit the creep curve of coal under water immersion. The coefficient of determination of the fitting results for the creep test of coal under 7 d, 14 d, and 30 d are 0.85, 0.86, and 0.83 respectively. This indicates that the fractional-order damage creep model based on the conformable derivative proposed in this paper can characterize the damage creep process of coal under water immersion.

5. Conclusions

The long-term stability of coal pillar dams is an essential issue for the safety operation of underground reservoirs. In order to develop a proper creep model for coal rock considering both the stress level and water-immersion time, this paper implemented creep experiments and analyzed the creep properties of water-immersed coal, then a fractional-order creep model was developed considering the immersion time and discussed based on the experiment data. The main conclusions are as follows:

(1) Water-immersion time has a significant influence on the elastoplastic performance of coal, exhibiting the longer water-immersion time, the lower elastic modulus and strength, and the degradation of the elastic modulus and strength, which is nonlinear to the increment of the water-immersion time.

(2) Both the stress level and water-immersion time reduce the elastic viscosity and plastic viscosity of coal with a slightly nonlinear relationship, thereby increasing its creep rate. Such a promoting effect is limited when the water-immersion time reaches to a certain period.

(3) A fractional-order derivative-based creep model was constructed to meet the deformation law of coal under the conditions of the variable stress level and water-immersion time. A verification of the creep model associated with the creep experiment suggests good agreement with the experiment curves, the stress levels, and the water-immersion time, showing the controlling role of the creep deformation of coal. It can well reflect the creep characteristics of the water-immersed coal at each stage of the stress levels.

Author Contributions: Conceptualization, G.L. and Q.W.; methodology, H.Y.; software, Z.L.; validation, G.L. and H.Y.; formal analysis, H.Y.; investigation, G.L.; resources, F.R. and Z.C.; data curation, F.R. and Z.C.; writing—original draft preparation, G.L.; writing—review and editing, H.Y.; visualization, Y.L.; funding acquisition, Z.L. and H.Y. All authors have read and agreed to the published version of the manuscript.

Funding: This research was funded by the National Natural Science Foundation of China (Grant No.52004090) and Hebei Natural Science Foundation (Grant No.E2021508026).

Institutional Review Board Statement: Not applicable.

Informed Consent Statement: Not applicable.

Data Availability Statement: The data supporting this study are included in the paper.

Conflicts of Interest: Author Qiqi Wanyan was employed by the company China National Petroleum Corporation. The remaining authors declare that the research was conducted in the absence of any commercial or financial relationships that could be construed as a potential conflict of interest.

References

1. Xie, H.; Zhao, J.; Zhou, H.; Ren, S.; Zhang, R. Secondary utilizations and perspectives of mined underground space. *Tunn. Undergr. Space Technol.* **2020**, *96*, 103129. [CrossRef]
2. Guo, P.; Wang, M.; Dang, G.; Zhu, T.; Wang, J.; He, M. Evaluation method of underground water storage space and thermal reservoir model in abandoned mine. *Rock Mech. Bull.* **2023**, *2*, 100044. [CrossRef]
3. Liu, F.; Li, S. Discussion on the new development and utilization of underground space resources of transitional coal mines. *J. China Coal Soc.* **2017**, *42*, 2205–2213.
4. Yong, X.; Chen, W.; Wu, Y.; Tao, Y.; Zhou, J.; He, J. A two-stage framework for site selection of underground pumped storage power stations using abandoned coal mines based on multi-criteria decision-making method: An empirical study in China. *Energy Convers. Manag.* **2022**, *260*, 115608. [CrossRef]
5. Xie, H.; Xu, W.; Liu, C.; Yang, X. The subversive idea and key technical prospects on underground hydraulic engineering. *Chin. J. Rock Mech. Eng.* **2018**, *37*, 781–791.
6. Qian, R.; Feng, G.; Guo, J.; Wang, P.; Jiang, H. Effects of water-soaking height on the deformation and failure of coal in uniaxial compression. *Appl. Sci.* **2019**, *9*, 4370. [CrossRef]
7. Wang, K.; Feng, G.; Bai, J.; Guo, J.; Shi, X.; Cui, B.; Song, C. Dynamic behaviour and failure mechanism of coal subjected to coupled water-static-dynamic loads. *Soil Dyn. Earthq. Eng.* **2022**, *153*, 107084. [CrossRef]
8. Fan, J.; Li, Z.; Feng, G.; Zhang, H.; Qi, C.; Zhang, J. Failure analysis of coal pillars and overburden from underground water reservoir under the mining-water invasion coupling effect. *Eng. Fail. Anal.* **2023**, *151* , 107406. [CrossRef]
9. Menéndez, J.; Schmidt, F.; Konietzky, H.; Fernández-Oro, J.M.; Galdo, M.; Loredo, J.; Díaz-Aguado, M.B. Stability analysis of the underground infrastructure for pumped storage hydropower plants in closed coal mines. *Tunn. Undergr. Space Technol.* **2019**, *94*, 103117. [CrossRef]
10. Colas, E.; Klopries, E.M.; Tian, D.; Kroll, M.; Selzner, M.; Bruecker, C.; Khaledi, K.; Kukla, P.; Preuße, A.; Sabarny, C.; et al. Overview of converting abandoned coal mines to underground pumped storage systems: Focus on the underground reservoir. *J. Energy Storage* **2023**, *73*, 109153. [CrossRef]
11. Zhang, C.; Wang, X.; Han, P.; Bai, Q.; Chen, J. Failure analysis of residual coal pillar under the coupling of mining stress and water immersion in the goaf underground water reservoir. *Environ. Earth Sci.* **2023**, *82*, 309. [CrossRef]
12. Bruno, G.; Tupputi, D.; Simeone, V. Geomechanical modelling and stability analysis of the shallow underground water reservoir 'Palombaro Lungo'(Matera-Italy). *Environ. Earth Sci.* **2023**, *82*, 302. [CrossRef]
13. Zhang, C.; Wang, F.; Bai, Q. Underground space utilization of coalmines in China: A review of underground water reservoir construction. *Tunn. Undergr. Space Technol.* **2021**, *107*, 103657. [CrossRef]
14. Lyu, X.; Chi, X.; Yang, K.; Yuan, L.; Fang, J.; Zhang, Z. Strength modeling and experimental study of coal pillar-artificial dam combination after wetting cycles. *J. Mater. Res. Technol.* **2023**, *25*, 3050–3060. [CrossRef]
15. Ju, J.; Li, Q.; Xu, J.; Wang, X.; Lou, J. Self-healing effect of water-conducting fractures due to water-rock interactions in undermined rock strata and its mechanisms. *Bull. Eng. Geol. Environ.* **2020**, *79*, 287–297. [CrossRef]
16. Liu, Q.; Sun, Y.; Li, J. Experimental study on seepage characteristics of Jurassic weakly cemented sandstone under water-rock interaction. *Geofluids* **2020**, *2020*, 8543687. [CrossRef]
17. Yao, Q.; Chen, T.; Tang, C.; Sedighi, M.; Wang, S.; Huang, Q. Influence of moisture on crack propagation in coal and its failure modes. *Eng. Geol.* **2019**, *258*, 105156. [CrossRef]
18. Depeng, M.; Yan, Z.; Chuanxiao, L. Creep behavior and acoustic emission characteristics of coal samples with different moisture content. *Acta Geodyn. Geomater.* **2018**, *15*, 405–412.
19. Chen, G.; Li, T.; Yang, L.; Zhang, G.; Lyu, P.; Teng, P. Mechanical properties and damage characteristics of coal-rock combined samples under water-rock interaction. *Coal Sci. Technol.* **2023**, *51*, 37–46. [CrossRef]

20. Song, H.; Zhong, Z.; Lin, B. Mechanical degradation model of porous coal with water intrusion. *Energy* **2023**, *278*, 127786. [CrossRef]
21. Yao, Q.; Chen, T.; Ju, M.; Liang, S.; Liu, Y.; Li, X. Effects of water intrusion on mechanical properties of and crack propagation in coal. *Rock Mech. Rock Eng.* **2016**, *49*, 4699–4709. [CrossRef]
22. Liu, Y.; Liu, C.; Kang, Y.; Wang, D.; Ye, D. Experimental research on creep properties of limestone under fluid–solid coupling. *Environ. Earth Sci.* **2015**, *73*, 7011–7018. [CrossRef]
23. Wang, Z.; Li, B.; Ren, C.; Li, J.; Cheng, Q.; Wu, X.; Yao, C. Energy-Driven Damage Constitutive Model of Water-Bearing Coal Under Triaxial Compression. *Rock Mech. Rock Eng.* **2023**, 1–20. [CrossRef]
24. Yi, S.; Zhang, Y.; Yi, H.; Li, X.; Wang, X.; Wang, Y.; Chu, T. Study on the instability activation mechanism and deformation law of surrounding rock affected by water immersion in goafs. *Water* **2022**, *14*, 3250. [CrossRef]
25. Yu, C.; Tang, S.; Tang, C.; Duan, D.; Zhang, Y.; Liang, Z.; Ma, K.; Ma, T. The effect of water on the creep behavior of red sandstone. *Eng. Geol.* **2019**, *253*, 64–74. [CrossRef]
26. Gao, Y.; Wei, W.; Hua, D.; Jiang, Q. Study on creep characteristics of mudstone with different initial water contents in soaking conditions and its engineering applications. *Bull. Eng. Geol. Environ.* **2022**, *81*, 380. [CrossRef]
27. Zhou, H.; Wang, C.; Han, B.; Duan, Z. A creep constitutive model for salt rock based on fractional derivatives. *Int. J. Rock Mech. Min. Sci.* **2011**, *48*, 116–121. [CrossRef]
28. Lyu, C.; Liu, J.; Ren, Y.; Liang, C.; Liao, Y. Study on very long-term creep tests and nonlinear creep-damage constitutive model of salt rock. *Int. J. Rock Mech. Min. Sci.* **2021**, *146*, 104873. [CrossRef]
29. Yang, C.; Daemen, J.; Yin, J.H. Experimental investigation of creep behavior of salt rock. *Int. J. Rock Mech. Min. Sci.* **1999**, *36*, 233–242. [CrossRef]
30. Kamdem, T.C.; Richard, K.G.; Béda, T. New description of the mechanical creep response of rocks by fractional derivative theory. *Appl. Math. Model.* **2022**, *116*, 624–635. [CrossRef]
31. Nishihara, M. Creep of shale and sandy-shale. *J. Geol. Soc. Jpn.* **1952**, *58*, 373–377. [CrossRef]
32. Feng, Y.Y.; Yang, X.J.; Liu, J.G.; Chen, Z.Q. A new fractional Nishihara-type model with creep damage considering thermal effect. *Eng. Fract. Mech.* **2021**, *242*, 107451. [CrossRef]
33. Wu, F.; Liu, J.F.; Wang, J. An improved Maxwell creep model for rock based on variable-order fractional derivatives. *Environ. Earth Sci.* **2015**, *73*, 6965–6971. [CrossRef]
34. Huang, P.; Zhang, J.; Damascene, N.J.; Dong, C.; Wang, Z. A fractional order viscoelastic-plastic creep model for coal sample considering initial damage accumulation. *Alex. Eng. J.* **2021**, *60*, 3921–3930. [CrossRef]
35. Hou, R.; Zhang, K.; Tao, J.; Xue, X.; Chen, Y. A nonlinear creep damage coupled model for rock considering the effect of initial damage. *Rock Mech. Rock Eng.* **2019**, *52*, 1275–1285. [CrossRef]
36. Zhou, H.; Wang, C.; Mishnaevsky, L.; Duan, Z.; Ding, J. A fractional derivative approach to full creep regions in salt rock. *Mech. Time-Depend. Mater.* **2013**, *17*, 413–425. [CrossRef]
37. Zhang, L.; Zhou, H.; Wang, X.; Wang, L.; Su, T.; Wei, Q.; Deng, T. A triaxial creep model for deep coal considering temperature effect based on fractional derivative. *Acta Geotech.* **2022**, *17*, 1739–1751. [CrossRef]
38. Deng, H.; Zhou, H.; Li, L. Fractional creep model of temperature-stress-time coupled damage for deep coal based on temperature-equivalent stress. *Results Phys.* **2022**, *39*, 105765. [CrossRef]
39. Yu, L.; Yao, Q.; Chong, Z.; Li, Y.; Xu, Q.; Liu, Z. Experimental study on the moisture migration and triaxial mechanical damage mechanisms of water-bearing coal samples. *Int. J. Rock Mech. Min. Sci.* **2022**, *160*, 105263. [CrossRef]
40. Guo, J.; Zhang, T.; Pan, H.; Wu, J. Experimental investigation of the creep damage evolution of coal rock around gas extraction boreholes at different water contents. *PLoS ONE* **2023**, *18*, e0278783. [CrossRef]
41. Ji, Z.; Jiang, P.; Yi, H.; Zhuo, Z.; Li, C.; Wu, Z. Application of two novel acoustic emission parameters on identifying the instability of granite. *Entropy* **2022**, *24*, 750. [CrossRef] [PubMed]
42. Chanard, K.; Nicolas, A.; Hatano, T.; Petrelis, F.; Latour, S.; Vinciguerra, S.; Schubnel, A. Sensitivity of acoustic emission triggering to small pore pressure cycling perturbations during brittle creep. *Geophys. Res. Lett.* **2019**, *46*, 7414–7423. [CrossRef]
43. Xu, T.; Zhou, G.; Heap, M.J.; Yang, S.; Konietzky, H.; Baud, P. The modeling of time-dependent deformation and fracturing of brittle rocks under varying confining and pore pressures. *Rock Mech. Rock Eng.* **2018**, *51*, 3241–3263. [CrossRef]
44. Yu, L.; Yao, Q.; Chong, Z.; Li, Y.; Xu, Q.; Xie, H.; Ye, P. Mechanical and micro-structural damage mechanisms of coal samples treated with dry–wet cycles. *Eng. Geol.* **2022**, *304*, 106637. [CrossRef]
45. Khalil, R.; Al Horani, M.; Yousef, A.; Sababheh, M. A new definition of fractional derivative. *J. Comput. Appl. Math.* **2014**, *264*, 65–70. [CrossRef]

Disclaimer/Publisher's Note: The statements, opinions and data contained in all publications are solely those of the individual author(s) and contributor(s) and not of MDPI and/or the editor(s). MDPI and/or the editor(s) disclaim responsibility for any injury to people or property resulting from any ideas, methods, instructions or products referred to in the content.